RESEARCH PAPER

Islets 7:4, e1107255; July/August 2015; © 2015 Taylor & Francis Group, LLC

Reactive oxygen and nitrogen species disturb Ca^{2+} oscillations in insulin-secreting MIN6 β-cells

Salvatore Antonucci[1,2], Alessia Tagliavini[3], and Morten Gram Pedersen[3,*]

[1]Department of Biomedical Sciences; University of Padua; Padua, Italy; [2]Venetian Institute of Molecular Medicine; Padua, Italy; [3]Department of Information Engineering; University of Padua; Padua, Italy

Keywords: calcium pumps, mathematical modeling, pulsatile insulin secretion, photosensitizer, ROS/RNS

Abbreviations: AlClPc, Aluminum Phthalocyanine Chloride; CICR, calcium-induced calcium release; CuFL, selective turn-on fluorescent NO reporter formed by a Cu(II) complex of a fluorescein modified with an appended metal-chelating ligand (FL); ER, endoplasmic reticulum; IP_3R, inositol triphospate receptor; MitoSOX, mitochondrial superoxide indicator; NO, nitric oxide; PMCA, plasma membrane Ca^{2+} ATPase; RNS, reactive nitrogen species; ROS, reactive oxygen species; RyR, ryanodine receptor; SERCA, Sarcoplasmic/endoplasmic reticulum Ca^{2+} ATPase; TEA, tetraethylammonium; Tg, thapsigargin.

Disturbances in pulsatile insulin secretion and Ca^{2+} oscillations in pancreatic β-cells are early markers of diabetes, but the underlying mechanisms are still incompletely understood. Reactive oxygen/nitrogen species (ROS/RNS) are implicated in reduced β-cell function, and ROS/RNS target several Ca^{2+} pumps and channels. Thus, we hypothesized that ROS/RNS could disturb Ca^{2+} oscillations and downstream insulin pulsatility. We show that ROS/RNS production by photoactivation of aluminum phthalocyanine chloride (AlClPc) abolish or accelerate Ca^{2+} oscillations in the MIN6 β-cell line, depending on the amount of ROS/RNS. Application of the sarcoplasmic/endoplasmic reticulum Ca^{2+} ATPase (SERCA) inhibitor thapsigargin modifies the Ca^{2+} response to high concentrations of ROS/RNS. Further, thapsigargin produces effects that resemble those elicited by moderate ROS/RNS production. These results indicate that ROS/RNS interfere with endoplasmic reticulum Ca^{2+} handling. This idea is supported by theoretical studies using a mathematical model of Ca^{2+} handling adapted to MIN6 cells. Our results suggest a putative link between ROS/RNS and disturbed pulsatile insulin secretion.

Introduction

Insulin is secreted from the pancreatic β-cells in distinct pulses[1,2] and disturbed pulsatile insulin release has been suggested to be an early marker of diabetes.[3] These bursts of insulin are driven by underlying oscillations in electrical activity and cytosolic Ca^{2+} levels, which periodically trigger Ca^{2+}-regulated exocytosis.[4] Importantly, secretory pulses are more effective than constant insulin levels in lowering plasma glucose levels.[3,5,6] In particular, hepatic signaling is highly sensitive to whether insulin is released in pulses,[7] leading to the suggestion that insulin resistance in the liver is secondary to disturbed pulsatile insulin release.[8] Thus, a deeper understanding of oscillatory β-cell activity and its disturbance has clinical relevance.

Disturbed insulin secretion and diabetes have been associated with β-cell damage caused by reactive oxygen species (ROS).[9] However, ROS have also been shown to exert a stimulating short-term effect on insulin release.[10] Hence, ROS may act as a double-edged sword: moderate and short-term elevations play a positive signaling role augmenting insulin secretion, but prolonged exposure to elevated ROS levels, characteristic of oxidative stress, are detrimental for the β-cells.[9,11] Similarly, reactive nitrogen species (RNS), such as nitric oxide (NO), have been shown to elevate Ca^{2+} levels and stimulate insulin secretion at low concentrations,[12] whereas high NO concentrations exert an inhibitory effect on β-cell function[12] and survival.[13]

ROS/RNS target various cellular mechanisms underlying insulin secretion,[9] and in particular components involved in Ca^{2+} handling.[14,15] For example ROS/RNS activate voltage-gated Ca^{2+} channels and endoplasmic reticulum (ER) release channels, such as the inositol triphospate receptors (IP_3Rs) and ryanodine receptors (RyRs). In addition, sarcoplasmic/endoplasmic reticulum Ca^{2+} ATPases (SERCAs) and plasma membrane Ca^{2+} ATPases (PMCAs) are inhibited by ROS/RNS. All these effects contribute to elevating the cytosolic Ca^{2+} concentration, which may trigger cell dysfunction.[16] Moreover, ROS/RNS effects on ER Ca^{2+} handling could lead to ER stress and consequent protein misfolding.[17] In addition, and of particular interest for the present study, ROS/RNS effects on the Ca^{2+} handling machinery might disturb Ca^{2+} oscillations and downstream pulsatile insulin release.

Aluminum phthalocyanine chloride (AlClPc) is a photosensitizer commonly used in photodynamic therapy experiments and clinical protocols; photoactivation of AlClPc induces chemical

*Correspondence to: Morten Gram Pedersen; Email: pedersen@dei.unipd.it
Submitted: 09/10/2015; Revised: 10/06/2015; Accepted: 10/06/2015
http://dx.doi.org/10.1080/19382014.2015.1107255

changes into neighboring molecules, which lead to ROS production,[18] as well as NO/RNS release.[19-21] Here we show that ROS/RNS production by AlClPc photoactivation accelerates or abolishes Ca^{2+} oscillations in the widely used insulin-secreting MIN6 β-cell line. To guide the interpretation of our results, we used a mathematical model of Ca^{2+} handling adapted to MIN6 cells. The model results support the notion that ROS/RNS effects on ER Ca^{2+} are insufficient to interrupt Ca^{2+} oscillations, and that inhibition of PMCA by high ROS/RNS levels could underlie the cessation of the periodic Ca^{2+} pattern seen at maximal AlClPc photoactivation.

Materials and Methods

Experiments

Cells

MIN6 β-cells ([22]; passages 19–40; a gift from Prof. L. Eliasson, LUDC, Malmö, Sweden) were grown in Dulbecco's modified Eagle's medium (DMEM) High glucose (4 g/L – 23 mM) and L-glutamine (0.58 g/L – 4 mM), supplemented with 15% heat-inactivated Fetal Bovine Serum (FBS), 75 mg/L penicillin, 50 mg/L streptomycin and maintained in a humidified incubator with 95% air and 5% CO2 at 37°C. Medium was changed every 2–3 d and cells were passed every 5–7 d when they were ~60% confluent.[22,23]

Imaging

Culture media, compounds and chemicals were all from Sigma Aldrich, except Fura-2 AM (Life Technologies, F-1221), MitoSOX (Life Technologies, M36008) and CuFl (see below).

Experiments were conducted at room temperature under constant flow perfusion with extracellular medium (ECM) at pH 7.4 (adjusted with NaOH). The ECM was composed of (in mM): 150 NaCl, 5 KCl, 1 MgCl, 10 Hepes, 2 NaPyr, 2 $CaCl_2$, and either 3 or 25 d-Glucose. In most experiments 15 mM Tetra Ethyl Ammonium (TEA, a K^+ channel blocker) Chloride was added to the ECM containing 25 mM d-Glucose. Where indicated, SERCA pumps were inhibited by the addition of 200 nM Thapsigargin.

Intracellular free Ca^{2+} concentration was tracked by fluorescence imaging using Fura-2 acetoxymethyl (AM) ester. MIN6 pseudoislets were placed on poly-L-lysine (0.1% for 2h) treated coverslips and incubated at 37°C in DMEM High Glucose (D5796) for a total time of 20 minutes with 5 μM Fura-2 AM, PluronicF-127 (0,01% w/v) and Sulfinpyrazione (250 μM). Pluronic (P2443) and Sulfinpyrazone (S9509) were used to prevent the complexation and secretion of dye. ROS production was obtained by photoactivation at 660 nm of AlClPc (363530). Min6 pseudoislets were incubated at 37°C in DMEM High Glucose for a total time of 1 hour with 10 μM AlClPc.

NO was monitored by fluorescence imaging using CuFL. The probe was prepared using the Nitric Oxide Sensor (Intracellular) Kit (Strem Chemicals, part No. 96–0293) by reacting the fluorescein-based ligand 2-{2-Chloro-6-hydroxy-5-[2-methylquinolin-8-ylamino)methyl]- 3-oxo-3H- xanthen-9-yl}benzoic acid (FL) with $CuCL_2$ in a 1:1 ratio in buffered aqueous solution. Min6 pseudoislets were incubated in ECM solution for a total time of 15 min at room temperature with 20 μM CuFl and then washed for 15 min with ECM solution.[24] ROS signaling was monitored with fluorescence imaging using MitoSOX. Min6 pseudoislets were incubated at 37°C in DMEM High glucose (D5796) without FBS for a total time of 15 minutes with 2.5 μM MitoSOX.

In experiments with Fura-2, specimens were excited alternately by 365 nm and 385 nm high power LEDs (Thorlabs, M365L2 - M385L2). In experiments with CuFl [24] (Lim et al., 2006), specimens were excited with 460 nm high efficacy 5W Dental Blue LED (Led Engine, LZ1–00DB00). In experiments with MitoSOX, specimens were excited with 530 nm high power LED (Thorlabs, M530L3). Phthalocyanine was photoactivated by 660 nm high power LED (Thorlabs, M660L3) filtered through a pair of polarizers to modulate the LED intensity. The fluorescence emission was selected by an emission filter (HQ 520/40, Chroma, Rockingham, VT) and the emitted fluorescence images were collected by a complementary metal-oxide semiconductor (CMOS) cooled camera (Pco.Edge) using a water immersion objective (40′, Lumplan FL, N.A.= 0.80; Olympus). To generate each frame, the 365 nm and 385 nm LEDs were activated in rapid sequence for 200 ms each and a fura-2 ratio image was generated every second. The 460 nm LED was activated for 100 ms and a CuFL intensity image was generated every second. The 530 nm LED was activated for 200 ms and a MitoSOX intensity image was generated every second. For pulsed-light experiments, the 660 nm LED was activated for 100 ms/pulse and 1 pulse/second.

Data analysis

Images were analyzed with software developed using the Matlab platform (Release 14, MathWorks, Inc., Natick, MA, USA). Ca^{2+} signals were measured as fura-2 emission ratio changes, $\Delta R = R(t) - R(0)$, where t is time, $R(t)$ is fura-2 emission intensity excited at 365 nm divided by the intensity excited at 385 nm, and $R(0)$ indicates pre–stimulus ratio.

Fura-2, CuFL and MitoSOX traces were generated by averaging pixel signals within regions of interest (ROIs) corresponding to individual cells. Traces were analyzed using an ad-hoc developed Matlab function that identifies local maxima. Function parameters were adjusted in order to discard noise fluctuations and retain only true Ca^{2+} oscillation peaks. The temporal occurrence of the peaks was used to calculate the time interval between 2 consecutive peaks (period). For each cell (ROI), peak period and amplitude values were averaged to obtain a single-cell value.

Statistical comparisons were done with unpaired t tests for samples with unequal variance.

Mathematical modeling

We used a mathematical model of oscillatory behavior in β-cells[25] to investigate the effects of TEA and modifications in

ER Ca^{2+} handling on Ca^{2+} oscillations. The model reproduces many observed patterns in mouse β-cells, and was here adapted to MIN6 cells.

The model includes 4 voltage-gated currents: a Ca^{2+} current (I_{Ca}), a delayed rectifier K^+ current (I_K), a Ca^{2+} - dependent K^+ current ($I_{K(Ca)}$), and an ATP-sensitive K^+ current ($I_{K(ATP)}$). The membrane potential V evolves in time according to Eq. A1. All currents are modeled as in.[25] The ratio ADP/ATP is allowed to vary (Eq. A3) according to evidence of ATP oscillations in MIN6 cells.[27] The model also includes Ca^{2+} dynamics in the cytosol and in the ER of MIN6 cells as described by Eq. A6. Influx into the ER, via SERCA pumps, and ER efflux are modeled according to Eq. A7. The ER Ca^{2+} release rate p_{ER} can be either constant, or an increasing function of cytosolic $[Ca^{2+}]$ (c) to simulate calcium-induced calcium release (CICR), which is operating in MIN6 cells.[28]

The main mechanism resulting in oscillatory behavior in the model is negative feedback of Ca^{2+} onto the ATP concentration, for example because of increased ATP consumption by Ca^{2+} pumps. Lower ATP levels lead to K(ATP)-channel opening and, eventually, to cessation of electrical activity and Ca^{2+} influx. Calcium is then removed from the cytosol, allowing ATP levels to rise, resulting in reduced K(ATP)-current, reappearance of electrical activity and increasing cytosolic Ca^{2+} levels due to Ca^{2+} influx.

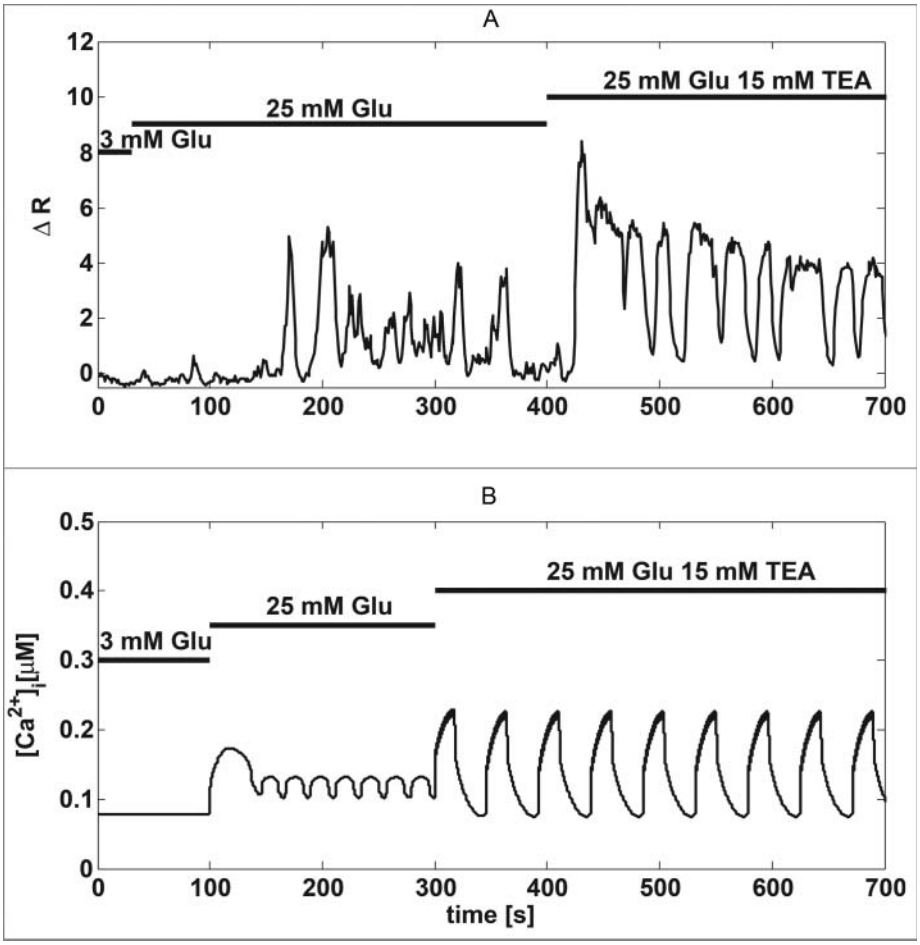

Figure 1. The K^+ channel antagonist TEA induces large amplitude Ca^{2+} oscillations. (**A**) Recording of Fura-2 fluorescence reporting Ca^{2+} concentrations in a MIN6 cell stimulated by glucose and TEA, as indicated. (**B**) Model simulation of the experiment in panel a). The increase in glucose from 3 mM to 25 mM was simulated by lowering g_{KATP} to 500 pS from 650 pS; TEA application was simulated by decreasing the K_v conductance (g_{Kv}) by ~80 %, from 41 nS to 8 nS.

For completeness, all expressions and parameters are given in the Appendix. Simulations were performed in the XPPAUT software[26] using the cvode solver.

Results

Glucose and TEA concur to evoke Ca^{2+} oscillations in MIN6 cells by blocking excessive K^+ currents

The MIN6 β-cell line[22] is widely used to investigate mechanisms underlying insulin secretion due to its good glucose responsiveness and relatively easy experimental handling.[22,23,29,30] It is well known that MIN6 cells exhibit irregular, small-amplitude Ca^{2+} oscillations when exposed to glucose, and that the addition of the K^+ channel antagonist tetraethylammonium (TEA) changes these fluctuations into large-amplitude and more regular oscillations (**Fig. 1A**; see also[23,31]). The period of the induced oscillations was typically 20–30 sec, similar to published results for MIN6 cells[23,30,31] and so-called fast Ca^{2+} oscillations observed in mouse islets.[32,33]

To obtain insight into this behavior, we used a mathematical model of oscillatory behavior in β-cells.[25] We assumed that, compared to pancreatic β cells in islets of Langerhans, MIN6 cells have larger K^+ currents,[31] which prevent large-amplitude oscillations. Our model suggests that this mechanism is plausible. Small-amplitude, high-frequency fluctuations were transformed into slower large-amplitude oscillations when the conductance of the K_v current was reduced by ~80% (**Fig. 1B**; see also[31]).

Phthalocyanine photoactivation leads to ROS and RNS production and increases cytosolic Ca^{2+} levels

To investigate the short-term effects of ROS/RNS on oscillatory Ca^{2+} dynamics in MIN6 cells, we loaded the cells with AlClPc. When photoexcited at 660 nm, AlClPc produces ROS in amounts depending on the intensity of the LED illumination as revealed by the ROS sensor MitoSOX (**Fig. 2A**). LED illumination *per se*, i.e., in the absence of AlClPc, did not produce

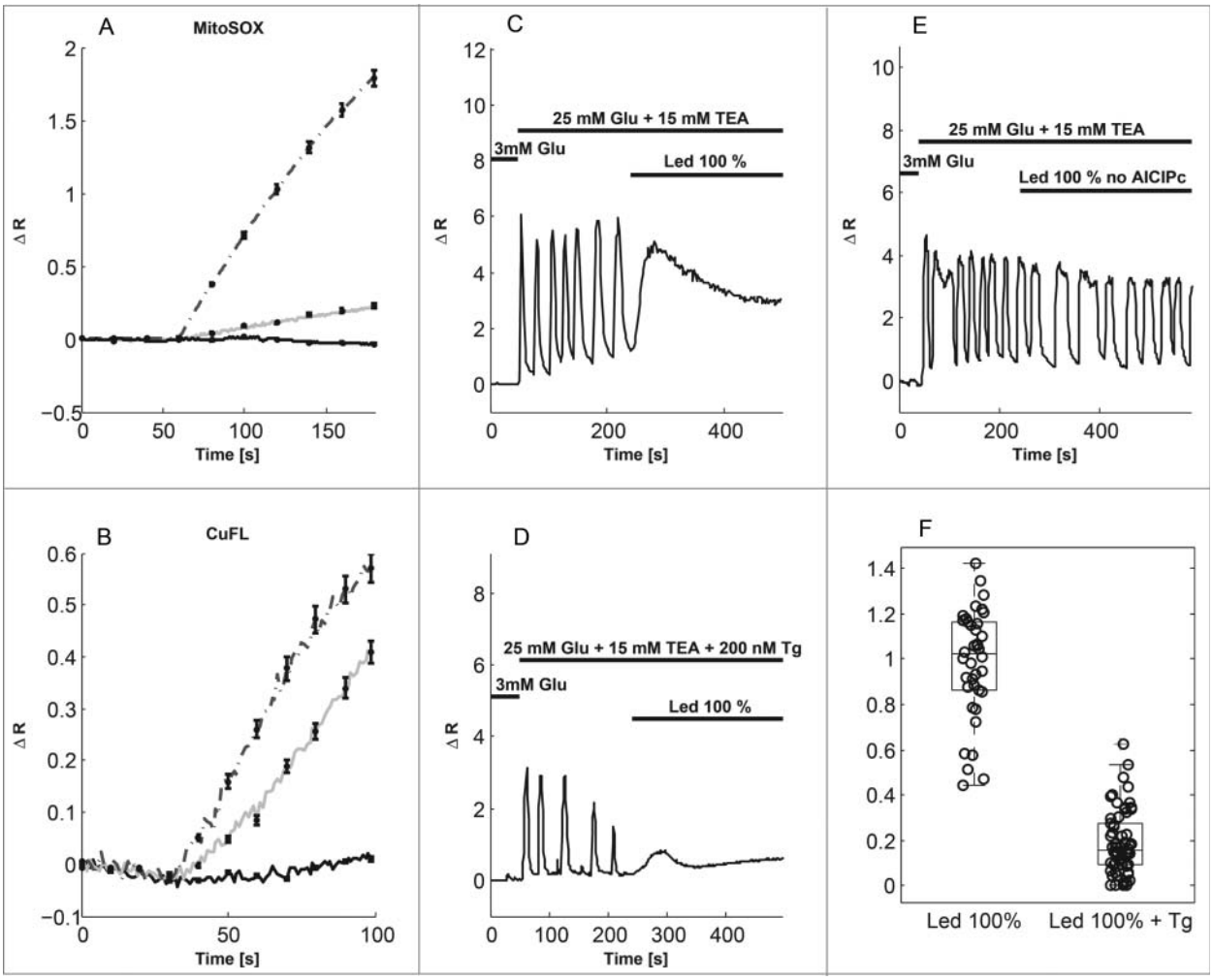

Figure 2. Photoactivation of phthalocyanine (AlClPc) produces ROS and RNS that interfere with Ca^{2+} oscillations in MIN6 cells. (**A**) ROS production by AlClPc photoactivation measured with the superoxide sensor MitoSOX (illumination from t = 60 s). The LED intensity was 100% (dashed curve) or 10% (grey curve). The full, black curve shows the ROS response to 100% LED illumination in the absence of AlClPc. (**B**) NO levels monitored with the sensor CuFL (illumination from t = 30 s) at 30% (full, black), 70% (grey) or 100% (dashed) LED intensity. Curves in panels a) and b) show the average signal, error bars indicate standard errors (n = 10-69 cells in 2-5 experiments per group). (**C**) Photoactivation of AlClPc with 100% LED intensity abolishes Ca^{2+} oscillations and results in a peak of $[Ca^{2+}]_c$. (**D**) In the presence of 200 nM Tg, the Ca^{2+} peak in response to 100% LED photoactivation is reduced. (**E**) In the absence of AlClPc, 100% LED illumination did not interfere with Ca^{2+} oscillations (representative of 37 cells in 4 experiments). (**F**) Summary of the Fura-2 (Ca^{2+}) peak normalized to oscillation amplitude in cells in the absence (ctrl, n = 38) and presence of Tg (n = 62).

ROS, nor result in any artifactual MitoSOX signal (**Fig. 2A**). Control experiments with HyPer, another ROS sensor, confirmed these results (**Fig. S1**). In addition, AlClPc photoactivation increased NO levels,[21] as reported by the selective fluorescent probe CuFL[21] (**Fig. 2B**; see also[19]). We found that ROS/RNS production by photoactivation of AlClPc at maximal (100%) LED intensity abolished Ca^{2+} oscillations in MIN6 cells. The Ca^{2+} concentration showed a peak and then settled at an intermediate level (**Fig. 2C**). When SERCA pumps were inhibited by thapsigargin (Tg) to prevent ER Ca^{2+} filling (**Fig. 2D**), the Ca^{2+} peak was substantially reduced (Ratio of peak to oscillation amplitude; ctrl: 0.98 ± 0.04 (n = 38), Tg: 0.19 ± 0.02 (n = 62), $p<0.001$, **Fig. 2F**). Control experiments in the absence of AlClPc showed that maximal LED illumination did not per se influence the Ca^{2+} oscillations (**Fig. 2E**). These observations suggest that the surge of cytosolic Ca^{2+} in response to ROS/RNS production is caused primarily by release of Ca^{2+} from the ER. Indeed, ROS/RNS are known to inhibit SERCA pumps and activate RyRs and IP_3Rs.[14,15]

Moderate levels of ROS/RNS modify Ca^{2+} oscillations

Having established that massive ROS/RNS production by AlClPc photoactivation abolishes Ca^{2+} oscillations in MIN6 cells, we turned our attention to the effects of moderate ROS/RNS levels. When photoactivating AlClPc with 10% LED intensity we observed that Ca^{2+} oscillations typically persisted, but with a modified profile.

Under control conditions, a step from 3 mM glucose to 25 mM glucose plus 15 mM TEA elicited a biphasic response consisting of a 1st phase lasting ~4–5 min with rapid oscillations

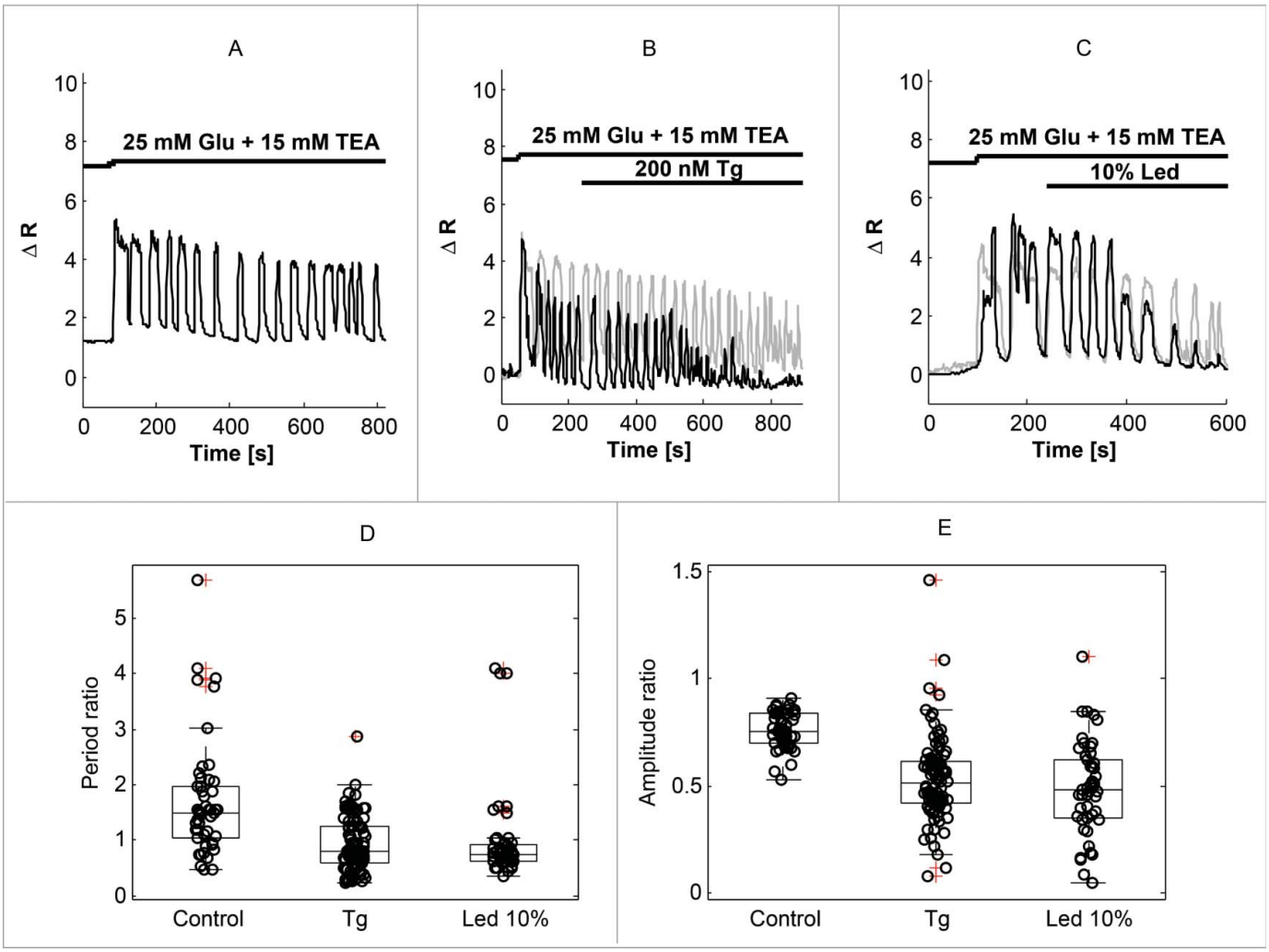

Figure 3. Thapsigargin (Tg) and moderate levels of ROS/RNS accelerate Ca^{2+} oscillations. (**A**) Example of Ca^{2+} trace in a MIN6 cell stimulated with 25 mM glucose and 15 mM TEA. (**B**) SERCA inhibition by Tg accelerates Ca^{2+} oscillations, and often reduces their amplitude (black trace). Two cells from 2 independent experiments with different amplitude responses are shown. (**C**) Moderate ROS/RNS production by 10% LED photoactivation of AlClPc result in modifications in Ca^{2+} oscillations similar to Tg application. Two synchronized cell from a single experiments with different amplitude responses are shown. (**D**) Summary of 2nd phase (after 240 sec) Ca^{2+} oscillation periods normalized to 1st phase (before 240 sec) periods in control conditions (n = 50), or in the presence of Tg (n = 102) or moderate ROS/RNS levels (n = 50) during the 2nd phase. (**E**) Summary of 2nd phase (after 240 sec) Ca^{2+} oscillation Fura-2 amplitudes normalized to 1st phase (before 240 sec) amplitudes in control conditions (n = 50), or in the presence of Tg (n = 102) or moderate ROS/RNS levels (n = 50) during the 2nd phase.

followed by a 2nd phase typically with slower oscillations (**Fig. 3A**). In contrast, the oscillations typically did not slow down when the second phase was perturbed by application of Tg (**Fig. 3B**) or photoactivation of AlClPc at 10% LED intensity (**Fig. 3C**) at t = 240 sec. Compared to control conditions, Tg or AlClPc photoactivation at 10% LED intensity resulted in a heterogeneous population of Ca^{2+} amplitude responses, which in some cells decreased substantially but in other showed behavior similar to the control patterns. This heterogeneity was observed when studying cells in different experiments (**Fig. 3B**) as well as for synchronized cells in the same experiment (**Fig. 3C**).

To handle cell heterogeneity, we normalized the single-cell 2nd phase oscillations period and amplitude to the 1st phase period and amplitude, respectively, of the same cell. This analysis revealed that the 2nd phase period increased by ~70% (ratio of 2nd to 1st phase periods 1.69 ± 0.14) under control conditions (**Fig. 3D**). In contrast, the period was unchanged when Tg or 10% LED photoactivation of AlClPc were present during the second phase (ratio of periods: 0.93±0.05 and 0.99±0.12, respectively; in both cases $p < 0.001$ vs. Control; p=0.22 Tg vs. 10% LED; **Fig. 3D**). The amplitude of the Fura-2 ratio signal was lower in the 2nd than in the 1st phase under control conditions (ratio of amplitudes 0.76±0.12). The reduction in 2^{nd} phase amplitude was greater in the presence of Tg or with 10% LED AlClPc photoactivation (ratio of amplitudes: 0.53±0.02 and 0.49±0.03, respectively; in both cases $p<0.001$ vs. control; p=0.20 Tg vs. 10%LED; **Fig. 3E**). However, there was

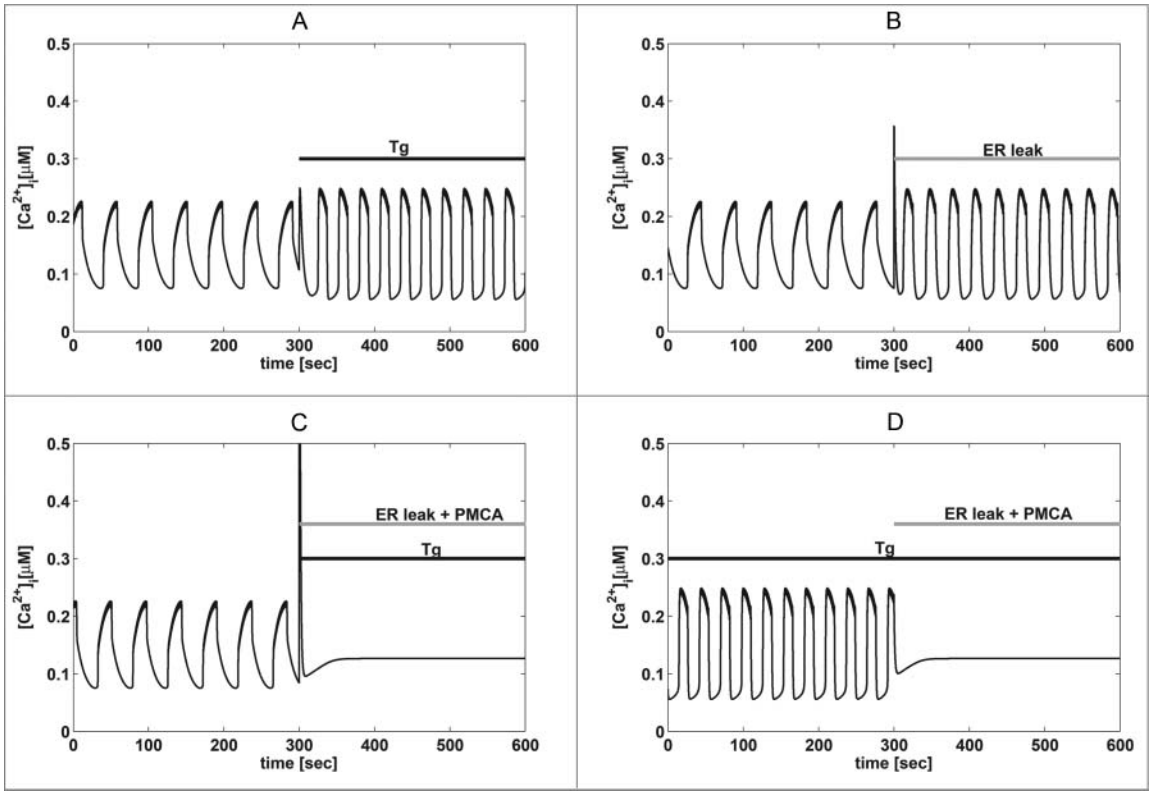

Figure 4. Mathematical modeling supports the experimental findings. (**A**) Model simulation showing acceleration of Ca^{2+} oscillations in response to Tg (k_{SERCA}=0 ms^{-1} as indicated by the bar "Tg"). (**B**) As in panel (**A**) but with increased ER Ca^{2+} release (p_{leak} multiplied by a factor 10, indicated by the bar). (**C**) Simulation of the combined effect of inhibition of PMCAs (k_{PMCA} lowered from 0.20 to 0.12 ms^{-1}), Tg application (as in panel **A**) and increased ER leak (as in panel **B**), which abolish Ca^{2+} oscillations as seen experimentally (**Figure 2B**). d) As in panel c), but with Tg present throughout as in **Figure 2C**, which removes the Ca^{2+} peak when ER leak and PMCA inhibition is simulated.

substantial cell-to-cell heterogeneity in the response to both Tg and to 10% LED AlClPc photoactivation, in particular with respect to the relative amplitude, which in many cases did not decrease more than in the control case (**Fig. 3B, C, E**). Nonetheless, the fact that Tg and 10% LED AlClPc photoactivation accelerate the Ca^{2+} oscillations and reduce their amplitude to a similar degree, suggest that their mechanism of action might be shared, i.e., inhibiting SERCA pumping, a well-known target of ROS/RNS,[14,15] and in accordance with our findings using 100% LED activation (**Fig. 2**).

Mathematical modeling suggests that modified ER Ca^{2+} handling and inhibition of PMCAs by ROS/RNS underlie acceleration and disappearance of Ca^{2+} oscillations

Altogether, the results described above indicate that ROS/RNS production by AlClPc and SERCA inhibition by Tg accelerate Ca^{2+} oscillations to a similar degree (**Fig. 3**). Moreover, the presence of Tg results in a reduction in the Ca^{2+} peak seen in response to high ROS/RNS levels (**Fig. 2**). These observations suggest that ROS/RNS modify Ca^{2+} oscillations via a reduction of ER Ca^{2+} levels. To test whether this interpretation is compatible with known β-cell Ca^{2+} handling mechanisms, we performed simulations with the model used to obtain insight into TEA-induced large-amplitude oscillations (**Fig. 1**). Consistent with our working hypothesis, the oscillatory behavior of the mathematical model accelerated when SERCA activity was lowered (**Fig. 4A**; see also[25]). Similarly, increasing Ca^{2+} release from the ER in the model (mimicking ROS/RNS activation of e.g. RyRs and IP3Rs;[14,15]) increased the frequency of the Ca^{2+} oscillations (**Fig. 4B**). However, the simulated amplitude was nearly unchanged by the presence of Tg or increased Ca^{2+} release. We note that some MIN6 cells showed amplitude responses to Tg or 10% LED AlClPc photoactivation that were similar to the control case (**Fig. 3**). Hence, these model simulations are more similar to this subgroup of MIN6 cells with respect to the effect on oscillation amplitude.

Of interest, the simulated modifications of ER Ca^{2+} handling were insufficient to abolish Ca^{2+} oscillations in the model. This result suggests that high levels of ROS/RNS, as produced by 100% LED AlClPc photoactivation (**Fig. 2**), also act on other components involved in the generation of rhythmic Ca^{2+} concentrations. For example, ROS/RNS are known to inhibit not only SERCA pumps, but also plasma membrane Ca^{2+} ATPases (PMCAs).[14,15] Our simulations confirmed that a reduction in the PMCA rate, together with

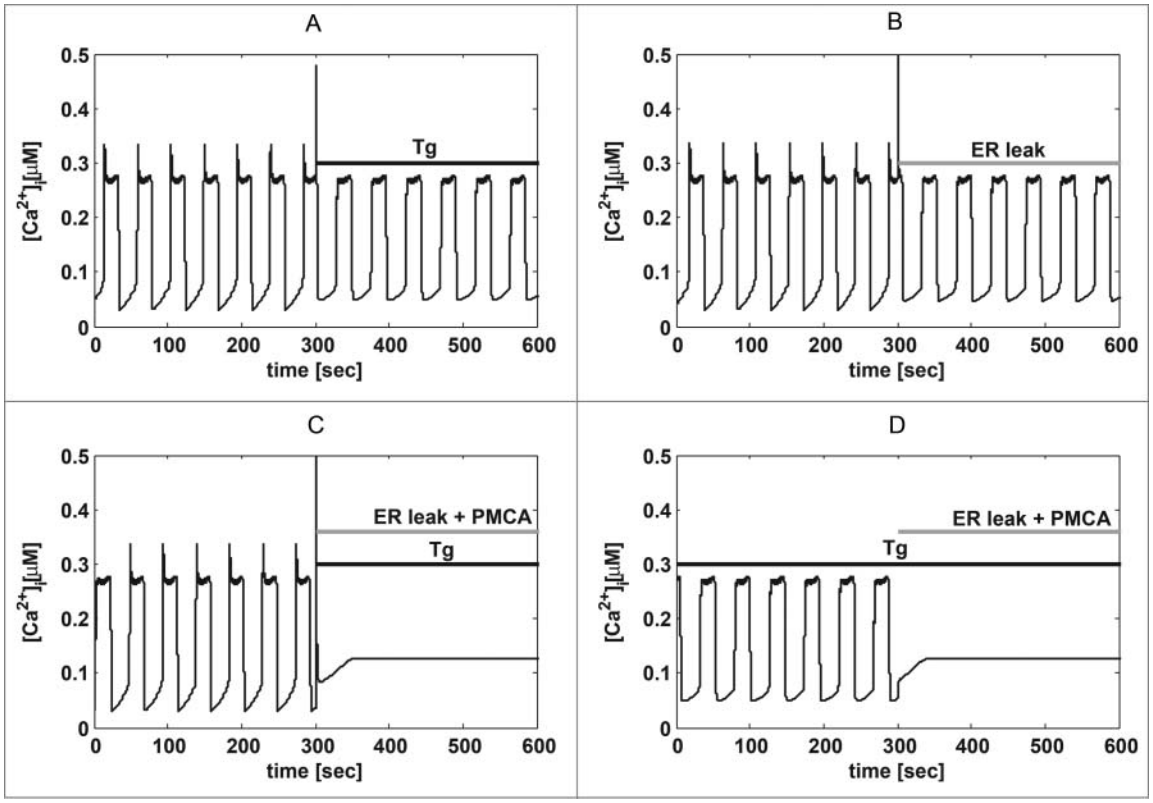

Figure 5. When CICR is playing a major role, causing a peak at the beginning of each Ca^{2+} rise, SERCA block ($k_{SERCA} = 0\ ms^{-1}$ as indicated by the bar "Tg") reduces Ca^{2+} oscillation amplitude. Simulations and panels as in **Figure 4**, but with $K_{cicr} = 0.3\ \mu M$, $p_{min} = 0.0018\ ms^{-1}$, $p_{max} = 0.1\ ms^{-1}$, $g_{k(Ca)} = 10$ pS, and $K_D = 0.2\ \mu M$. All other parameters were changed as described for **Figure 4**.

reduced SERCA activity and increased ER Ca^{2+} leak, could abolish Ca^{2+} oscillations (**Fig. 4C**). In agreement with experiments (**Fig. 2**), the presence of Tg before increasing ROS/RNS levels reduced the Ca^{2+} peak in our simulations (**Fig. 4D**). Thus, the model suggests that moderate ROS/RNS levels mainly act on ER Ca^{2+} handling, while high ROS/RNS concentrations might also inhibit PMCAs and thus abolish Ca^{2+} oscillations.

Discussion

It has been proposed that reactive oxygen species (ROS) act as a double-edged sword in β-cells.[11] Similarly, reactive nitrogen species (RNS) have beneficial or detrimental effects on β-cell function depending on their levels.[12] In agreement with this tenet we show here that massive ROS/RNS production by photoactivation of AlClPc at maximal (100%) LED intensity abolished Ca^{2+} oscillations in MIN6 β-cells (**Fig. 2**), while moderate ROS/RNS production (10% LED) accelerated the periodic Ca^{2+} excursions (**Fig. 3**). Since regular Ca^{2+} oscillations are a hallmark of healthy β-cell function,[4] our results suggest that massive ROS/RNS production lead to immediate β-cell dysfunction, whereas moderate ROS/RNS levels might have a slightly positive effect on the Ca^{2+} behavior since oscillations are more frequent. An interesting possibility is that dynamic control of ROS/RNS levels contributes to shaping physiological Ca^{2+} oscillations in β-cells.

Based on our experimental results, we suggest that moderate ROS/RNS levels could influence Ca^{2+} oscillations via inhibition of SERCA pumps and/or by increasing activity of ER release channels (IP3Rs/RyRs), all known targets of ROS/RNS.[14,15] The molecular mechanisms involved in ROS/RNS action include amino acid redox modifications; the typical targets are thiol groups of cysteine residues, albeit other amino acids such as arginine, lysine and methionine residues can also react with ROS/RNS.[14,34] Current hypotheses about the inactivation of PMCAs by ROS/RNS propose an alteration of PMCA Tyr589, Met622 and Met831 residues.[14] SERCA activity has been shown to be inhibited by ROS/RNS modification of cysteine (and tyrosine) residues.[14]

Model simulations support this hypothesis. In addition, the model suggests that high amounts of ROS/RNS also act on Ca^{2+} handling components at the plasma membrane, e.g., by inhibiting PMCAs – another ROS/RNS target,[14,15] which abolishes Ca^{2+} oscillations. Interestingly, it has been reported that SERCA is more sensitive to ROS than PMCA[35] in line with our findings.

The limited knowledge of MIN6 cell electrophysiology prevents the construction of a bottom-up, data-driven model, in contrast to was has been accomplished for example for human β-cells.[36-38] We included calcium-induced calcium release (CICR) in the model, since MIN6 cells are known to have

RyRs.[39] The reduced Ca^{2+} amplitude seen in experiments with Tg also indicates that CICR is playing a role in MIN6 cells. In contrast, in mouse islets Tg increases the amplitude of cytosolic Ca^{2+} oscillations[40] since the ER no longer takes up Ca^{2+}. In MIN6 cells, the ER likely functions both as a sink (due to SERCA) and a source (due to CICR) when $[Ca^{2+}]_c$ increases. The varying strengths of these 2 mechanisms likely underlie the heterogeneity seen in the amplitude responses to Tg and moderate ROS/RNS levels (**Fig. 3e**). Indeed, augmenting the role of CICR in our model can lead to reduced Ca^{2+} amplitude in response to SERCA block (**Fig. 5**). Further, the conclusions drawn from **Figure 4** remain valid also when CICR is active (**Fig. 5**).

In summary, we show that ROS/RNS can abolish or accelerate Ca^{2+} oscillations in insulin secreting cells, which might have important consequences for the disturbances of oscillatory β-cell function seen in early stages of diabetes. Our experiments and model simulations suggest that moderate ROS/RNS levels act on ER Ca^{2+} handling mechanisms, whereas higher levels of ROS/RNS also target other components involved in creating oscillatory behavior in insulin secreting cells.

Acknowledgments

We thank Prof. Lena Eliasson, Lund University Diabetes Center, Malmö, Sweden for the gift of MIN6 cells, Prof. Fabio Di Lisa, University of Padua, Italy, for the gift of HyPer, and Prof. Fabio Mammano, Venetian Institute of Molecular Medicine, Padua, Italy, for use of laboratory and microscopy facilities and technical assistance.

Funding

This work was supported by the University of Padova (PRAt 2012, and the Strategic Research Project 2012 "DYCENDI" to MGP).

Authors' Contributions

SA performed experiments, analyzed data, prepared figures, drafted and corrected the manuscript; AT analyzed data, developed the mathematical model, performed simulations and prepared figures; MGP designed and supervised model development, simulations and experiments, analyzed data, and wrote the manuscript. All authors gave final approval for publication.

Disclosure of Potential Conflicts of Interest

No potential conflicts of interest were disclosed.

Supplemental Material

Supplemental data for this article can be accessed on the publisher's website.

References

1. Gilon P, Shepherd RM, Henquin JC. Oscillations of secretion driven by oscillations of cytoplasmic Ca2+ as evidences in single pancreatic islets. J Biol Chem 1993 Oct 25; 268(30):22265-8; PMID:8226733
2. Ritzel RA, Veldhuis JD, Butler PC. Glucose stimulates pulsatile insulin secretion from human pancreatic islets by increasing secretory burst mass: dose-response relationships. J Clin Endocrinol Metab 2003 Feb; 88 (2):742-7; PMID:12574208
3. Pørksen N. The in vivo regulation of pulsatile insulin secretion. Diabetologia 2002 Jan; 45(1):3-20; PMID:11845219
4. Tengholm A, Gylfe E. Oscillatory control of insulin secretion. Mol Cell Endocrinol 2009 Jan 15; 297(1-2):58-72; PMID:18706473
5. Matthews DR, Naylor BA, Jones RG, Ward GM, Turner RC. Pulsatile insulin has greater hypoglycemic effect than continuous delivery. Diabetes 1983 Jul; 32 (7):617-21; PMID:6134649
6. Paolisso G, Scheen AJ, Giugliano D, Sgambato S, Albert A, Varricchio M, D'Onofrio F, Lefebvre PJ. Pulsatile insulin delivery has greater metabolic effects than continuous hormone administration in man: importance of pulse frequency. J Clin Endocrinol Metab 1991 Mar; 72(3):607-15.
7. Komjati M, Bratusch-Marrain P, Waldhäusl W. Superior efficacy of pulsatile versus continuous hormone exposure on hepatic glucose production in vitro. Endocrinology 1986 Jan; 118(1):312-9; PMID:3000741
8. Matveyenko AV, Liuwantara D, Gurlo T, Kirakossian D, Dalla Man C, Cobelli C, White MF, Copps KD, Volpi E, Fujita S, et al. Pulsatile portal vein insulin delivery enhances hepatic insulin action and signaling. Diabetes 2012 Sep; 61(9):2269-79; PMID:22688333
9. Supale S, Li N, Brun T, Maechler P. Mitochondrial dysfunction in pancreatic β cells. Trends Endocrinol Metab 2012 Sep; 23(9):477-87; PMID:22766318
10. Pi J, Bai Y, Zhang Q, Wong V, Floering LM, Daniel K, Reece JM, Deeney JT, Andersen ME, et al. Reactive oxygen species as a signal in glucose-stimulated insulin secretion. Diabetes 2007 Jul; 56(7):1783-91; PMID:17400930
11. Collins S, Pi J, Yehuda-Shnaidman E. Uncoupling and reactive oxygen species (ROS)–a double-edged sword for β-cell function? "Moderation in all things". Best Pract Res Clin Endocrinol Metab 2012 Dec; 26 (6):753-8; PMID:23168277
12. Kaneko Y, Ishikawa T, Amano S, Nakayama K. Dual effect of nitric oxide on cytosolic Ca2+ concentration and insulin secretion in rat pancreatic beta-cells. Am J Physiol Cell Physiol 2003 May; 284(5):C1215-22; PMID:12529241
13. Bedoya FJ, Salguero-Aranda C, Cahuana GM, Tapia-Limonchi R, Soria B, Tejedo JR. Regulation of pancreatic β-cell survival by nitric oxide: clinical relevance. Islets 2012 Jan; 4(2):108-18; PMID:22614339
14. Hidalgo C, Donoso P. Crosstalk between calcium and redox signaling: from molecular mechanisms to health implications. Antioxid Redox Signal 2008 Jul; 10 (7):1275-312; PMID:18377233
15. Feissner RF, Skalska J, Gaum WE, Sheu S-S. Crosstalk signaling between mitochondrial Ca2+ and ROS. Front Biosci (Landmark Ed.) 2009 Jan; 14:1197-218; PMID:19273125
16. Bernardi P, Rasola A. Calcium and cell death: the mitochondrial connection. Subcell Biochem 2007 Jan; 45:481-506; PMID:18193649
17. Tang C, Koulajian K, Schuiki I, Zhang L, Desai T, Ivovic A, Wang P, Robson-Doucette C, Wheeler MB, Minassian B, et al. Glucose-induced beta cell dysfunction in vivo in rats: link between oxidative stress and endoplasmic reticulum stress. Diabetologia 2012 May; 55(5):1366-79; PMID:22396011; http://dx.doi.org/10.1007/s00125-012-2474-8
18. Foote CS. Definition of type I and type II photosensitized oxidation. Photochem Photobiol 1991 Nov; 54 (5):659; PMID:1798741; http://dx.doi.org/10.1111/j.1751-1097.1991.tb02071.x
19. Gupta S, Ahmad N, Mukhtar H. Involvement of nitric oxide during phthalocyanine (Pc4) photodynamic therapy-mediated apoptosis. Cancer Res 1998 May 1; 58 (9):1785-8; PMID:9581812
20. Silva VHC, Martins MP, de Oliveira HCB, Camargo AJ. Theoretical investigation of nitric oxide interaction with aluminum phthalocyanine. J Mol Graph Model 2011 Apr; 29(6):777-83; PMID:21342778; http://dx.doi.org/10.1016/j.jmgm.2010.10.008
21. Calì B, Ceolin S, Ceriani F, Bortolozzi M, Agnellini HR, Zorzi V, Predonzani A, Bronte V, Molon B, Mammano F. Critical role of gap junction communication , calcium and nitric oxide signaling in bystander responses to focal photodynamic injury. Oncotarget 2015 Mar, 6(12): 10161-74; PMID:25868859; http://dx.doi.org/10.18632/oncotarget.3553
22. Ishihara H, Asano T, Tsukuda K, Katagiri H, Inukai K, Anai M, Kikuchi M, Yazaki Y, Miyazaki JI, Oka Y. Pancreatic beta cell line MIN6 exhibits characteristics of glucose metabolism and glucose-stimulated insulin secretion similar to those of normal islets. Diabetologia 1993 Nov; 36(11):1139-45; PMID:8270128; http://dx.doi.org/10.1007/BF00401058
23. Landa LR, Harbeck M, Kaihara K, Chepurny O, Kitiphongspattana K, Graf O, Nikolaev VO, Lohse MJ, Holz GG, Roe MW. Interplay of Ca2+ and cAMP signaling in the insulin-secreting MIN6 beta-cell line. J Biol Chem 2005 Sep 2; 280(35):31294-302; PMID:15987680; http://dx.doi.org/10.1074/jbc.M505657200
24. Lim MH, Xu D, Lippard SJ. Visualization of nitric oxide in living cells by a copper-based fluorescent probe. Nat Chem Biol 2006 Jul; 2(7):375-80;

PMID:16732295; http://dx.doi.org/10.1038/nchembio794
25. Bertram R, Sherman A. A calcium-based phantom bursting model for pancreatic islets. Bull Math Biol 2004 Sep; 66(5):1313-44; PMID:15294427; http://dx.doi.org/10.1016/j.bulm.2003.12.005
26. Ermentrout B. Simulating, Analyzing, and Animating Dynamical Systems: A Guide to XPPAUT for Researchers and Students. SIAM Books, Philadelphia, 2002.
27. Li J, Shuai HY, Gylfe E, Tengholm A. Oscillations of sub-membrane ATP in glucose-stimulated beta cells depend on negative feedback from Ca(2+). Diabetologia 2013 Jul; 56(7):1577-86; PMID:23536115; http://dx.doi.org/10.1007/s00125-013-2894-0
28. Varadi A, Rutter GA. Dynamic Imaging of Endoplasmic Reticulum Ca2+ Concentration in Insulin-Secreting MIN6 Cells Using Recombinant Targeted Cameleons: Roles of Sarco(endo)plasmic Reticulum Ca2+-ATPase (SERCA)-2 and Ryanodine Receptors. Diabetes 2002 Feb 1; 51(Supplement 1):S190-201; PMID:11815480; http://dx.doi.org/10.2337/diabetes.51.2007.S190
29. MacDonald PE, Wheeler MB. Voltage-dependent K (+) channels in pancreatic beta cells: role, regulation and potential as therapeutic targets. Diabetologia 2003 Aug; 46(8):1046-62; PMID:12830383; http://dx.doi.org/10.1007/s00125-003-1159-8
30. Hraha TH, Bernard AB, Nguyen LM, Anseth KS, Benninger RKP. Dimensionality and size scaling of coordinated Ca(2+) dynamics in MIN6 β-cell clusters. Biophys J 2014 Jan 7; 106(1):299-309; PMID:24411262; http://dx.doi.org/10.1016/j.bpj.2013.11.026
31. MacDonald PE, Sewing S, Wang J, Joseph JW, Smukler SR, Sakellaropoulos G, Wang J, Saleh MC, Chan CB, Tsushima RG, et al. Inhibition of Kv2.1 voltage-dependent K+ channels in pancreatic beta-cells enhances glucose-dependent insulin secretion. J Biol Chem 2002 Nov 22; 277(47):44938-45; PMID:12270920; http://dx.doi.org/10.1074/jbc.M205532200
32. Liu YJ, Tengholm a, Grapengiesser E, Hellman B, Gylfe E. Origin of slow and fast oscillations of Ca2+ in mouse pancreatic islets. J Physiol 1998 Apr 15; 508 Pt 2:471-81; PMID:9508810; http://dx.doi.org/10.1111/j.1469-7793.1998.471bq.x
33. Bertram R, Sherman A, Satin LS. Metabolic and electrical oscillations: partners in controlling pulsatile insulin secretion. Am J Physiol Endocrinol Metab 2007; 293:E890-900; PMID:17666486; http://dx.doi.org/10.1152/ajpendo.00359.2007
34. Bogeski I, Kappl R, Kummerow C, Gulaboski R, Hoth M, Niemeyer BA. Redox regulation of calcium ion channels: chemical and physiological aspects. Cell Calcium 2011 Nov; 50(5):407-23; PMID:21930299; http://dx.doi.org/10.1016/j.ceca.2011.07.006
35. Grover AK, Samson SE. Effect of superoxide radical on Ca2+ pumps of coronary artery. Am J Physiol 1988 Sep; 255(3 Pt 1):C297-303
36. Pedersen MG. A biophysical model of electrical activity in human β-cells. Biophys J 2010 Nov 17; 99 (10):3200-7; PMID:21081067; http://dx.doi.org/10.1016/j.bpj.2010.09.004
37. Riz M, Braun M, Pedersen MG. Mathematical modeling of heterogeneous electrophysiological responses in human β-cells. PLoS Comput Biol 2014 Jan; 10(1):e1003389; PMID:24391482; http://dx.doi.org/10.1371/journal.pcbi.1003389
38. Riz M, Braun M, Wu X, Pedersen MG. Inwardly rectifying Kir2.1 currents in human β-cells control electrical activity: Characterisation and mathematical modelling. Biochem Biophys Res Commun 2015 Apr 3; 459 (2):284-7; PMID:25727015; http://dx.doi.org/10.1016/j.bbrc.2015.02.099
39. Varadi A, Rutter GA. Dynamic imaging of endoplasmic reticulum Ca2+ concentration in insulin-secreting MIN6 Cells using recombinant targeted cameleons: roles of sarco(endo)plasmic reticulum Ca2+-ATPase (SERCA)-2 and ryanodine receptors. Diabetes 2002 Feb; 51 Suppl 1:S190-201; PMID:11815480; http://dx.doi.org/10.2337/diabetes.51.2007.S190
40. Gilon P, Arredouani A, Gailly P, Gromada J, Henquin JC. Uptake and release of Ca2+ by the endoplasmic reticulum contribute to the oscillations of the cytosolic Ca2+ concentration triggered by Ca2+ influx in the electrically excitable pancreatic B-cell. J Biol Chem 1999 Jul 16; 274(29):20197-205; PMID:10400636; http://dx.doi.org/10.1074/jbc.274.29.20197

Appendix: Model equations and parameters

For completeness we report all expressions and parameters of the mathematical model here, for more details see Bertram and Sherman.[25] The equations of the model for the membrane potentials V is

$$\frac{dV}{dt} = -\frac{(I_{Ca} + I_K + I_{K(Ca)} + I_{K(ATP)})}{C_m} \tag{A1}$$

where C_m is the membrane capacitance. The currents are modeled as

$$\begin{aligned} I_{Ca} &= g_{Ca} m_\infty(V)(V - V_{Ca}) \\ I_K &= g_K n (V - V_{Ca}) \\ I_{K(Ca)} &= g_{K(Ca)} \omega (V - V_K) \\ I_{K(ATP)} &= g_{K(ATP)} (V - V_K) \end{aligned} \tag{A2}$$

where the delayed rectifier activation, n, and the nucleotide ratio a are given by

$$\begin{aligned} \frac{dn}{dt} &= \frac{n_\infty(V) - n}{\tau_n} \\ \frac{da}{dt} &= \frac{a_\infty(c) - a}{\tau_a} \end{aligned} \tag{A3}$$

The equilibrium functions are described with Boltzmann functions,

$$\begin{aligned} m_\infty(V) &= \frac{1}{1 + e^{\left(\frac{v_m - V}{s_m}\right)}} \\ n_\infty(V) &= \frac{1}{1 + e^{\left(\frac{v_n - V}{s_n}\right)}} \\ a_\infty(V) &= \frac{1}{1 + e^{\left(\frac{r - c}{s_a}\right)}} \end{aligned} \tag{A4}$$

The variable ω is the fraction of K(Ca) channels activated by cytosolic Ca^{2+}.

$$\omega = \frac{c^5}{c^5 + {k_D}^5} \tag{A5}$$

where k_D is the Ca^{2+} level giving half-maximal activation of the K(Ca) current. The differential equations for the cytosolic Ca^{2+} and the ER Ca^{2+} are

$$\begin{aligned} \frac{dc}{dt} &= f_{cyt}(J_{mem} + J_{ER}) \\ \frac{dc_{ER}}{dt} &= f_{er}(V_{cyt}/V_{ER}) J_{ER} \end{aligned} \tag{A6}$$

Here, J_{mem} is the Ca^{2+} flux through the plasma membrane, f_{cyt} is the fraction of free to total Ca^{2+}, and f_{ER} is the fraction of free Ca^{2+} in the ER. J_{ER} is the total efflux from the ER. These fluxes are given by

$$\begin{aligned} J_{mem} &= -(\alpha I_{Ca} + k_{PMCA} c) \\ J_{ER} &= J_{leak} - J_{SERCA} \\ J_{SERCA} &= k_{SERCA} \\ J_{leak} &= p_{ER}(c_{ER} - c) \end{aligned} \tag{A7}$$

where α converts units of current to unit of flux, k_{PMCA} and k_{SERCA} are the rate constants for the plasma membrane Ca^{2+} ATPase pump (PMCA) and the ER membrane Ca^{2+} ATPase pump (SERCA), respectively. The release rate p_{ER} is

$$p_{ER} = p_{\min} + \frac{p_{\max} - p_{\min}}{1 + \left(\frac{K_{cicr}}{c}\right)^2} \tag{A8}$$

where the parameter K_{cicr} determines the amount of calcium-induced calcium release (CICR), which is absent for $K_{cicr} = 0$ μM. All parameters are given in Table A1.

Table A1. Default parameter values of the mathematical model used to simulate MIN6 cells in the presence of 25 mM glucose and 15 mM TEA

Parameter			Parameter		
g_{Ca}	1200	pS	s_a	0.1	μM
V_{Ca}	25	mV	τ_a	50000	ms
v_m	−20	mV	α	4.5×10^{-6}	fA^{-1} μM ms^{-1}
s_m	12	mV	f_{cyt}	0.01	
g_K	8000	pS	f_{er}	0.01	
V_K	−75	mV	k_{PMCA}	0.2	ms^{-1}
v_n	−16	mV	k_{SERCA}	0.4	ms^{-1}
s_n	5	mV	V_{cyt}/V_{er}	5	
τ_n	16	ms	p_{min}	5×10^{-4}	ms^{-1}
$g_{K(Ca)}$	100	pS	p_{max}	5×10^{-3}	ms^{-1}
k_D	0.3	μM	K_{cicr}	0.0	μM
$g_{K(ATP)}$	500	pS	C_m	5300	fF
r	0.14	μM			